Analytical methods

3. Analytical Methods

3.1 Identification of Paclitaxel (PTX) by FTIR

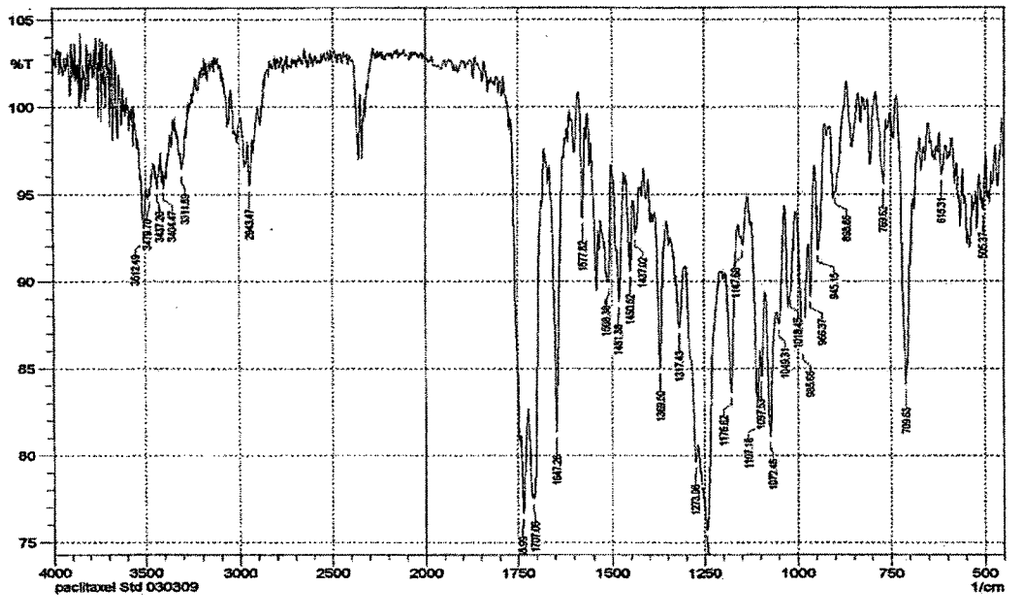

Figure 3. 1: FTIR spectra of paclitaxel

The FTIR spectra of PTX complies with the reference spectra of PTX.

3.2 Estimation of PTX

The UV-Visible method of estimation of PTX in different formulations was developed based on the observation that PTX showed strong absorbance in the UV region of the electromagnetic spectrum at wavelength maxima of 230nm in various solvents like ethanol, acetonitrile, chloroform: methanol (1:9) and pH 7.4 phosphate buffer containing 20% w/v ethanol. Also HPLC method for determination of PTX in plasma and different biological tissues (brain, heart, liver, spleen, tumor etc) was developed.

3.2.1 UV-Visible Spectroscopy

All spectroscopic estimations were performed on a Shimadzu UV Visible spectrophotometer (UV 1700, Shimadzu Coporation, Japan) at a wavelength of 230nm.

Preparation of standard stock solutions

Stock solution of PTX is to be prepared by accurately weighing 10mg of PTX in 10mL solvent (1000µg/mL PTX) and for pH 7.4 phosphate buffer containing 20% ethanol 10mg PTX in 200mL of buffer (50µg/mL PTX).

Preparation of calibration curve

Suitable aliquots of standard stock solution were accurately measured and transferred to the 10 ml of volumetric flask to prepare a working stock solution of PTX (100 µg/mL). Suitable aliquots of working stock solution were accurately measured and transferred to the 10 ml of volumetric flasks. The final volume was made up to 10 ml with the solvent (acetonitrile and chloroform: methanol (1:9)) to give final concentrations of 2, 4, 6, 8, 10, 20, 30, 40 µg/mL and the absorbance measured on a UV-Visible spectrophotometer (Shimadzu, Japan) against suitable blank at 230nm. For pH 7.4 phosphate buffer containing 20% ethanol the standard solution prepared were 5, 10, 15, 20, 25, 30 µg/mL and absorbance measured at 230nm. The above procedure was repeated four times and results recorded in the following tables.

Accuracy and Precision

In order to determine the accuracy and precision of the developed method, known amounts of PTX (4µg/mL, 20µg/mL and 40µg/mL) were subjected to recovery studies as per the procedure described above in different solvents.

Table 3. 1: Calibration Curve of PTX in $CHCl_3$: MeOH

Concentration (µg/ml)	Mean Absorbance ± SD (n=4)
2	0.126 ± 0.031
4	0.177 ± 0.014
6	0.246 ± 0.006
8	0.312 ± 0.007
10	0.384 ± 0.008
20	0.731 ± 0.012
30	1.101 ± 0.027
40	1.423 ± 0.026

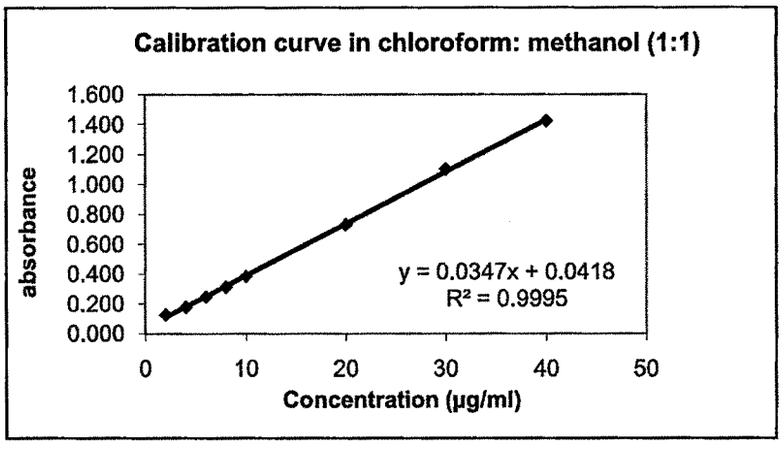

Figure 3. 2: Regressed calibration curve of PTX in $CHCl_3$: MeOH

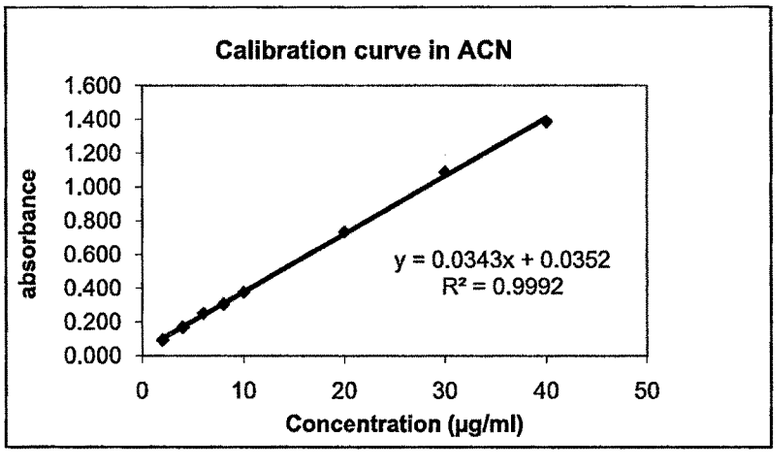

Figure 3. 3: Regressed calibration curve of PTX in ACN

Table 3. 2: Evaluation of accuracy & precision of the estimation method of PTX in $CHCl_3$: MeOH

Theoretical Concentration of PTX (µg/mL)	Determined Value (µg/mL) ± SD	Coefficient of variance (CV)	SEM ($SD/n^{1/2}$)	Confidence limits*
4	3.970 ± 0.085	0.007	0.043	3.970 ± 0.136
20	20.00 ± 0.184	0.034	0.092	20.00 ± 0.292
40	40.09 ± 0.051	0.003	0.026	40.09 ± 0.082

* At 95% Confidence level; t_{tab} = 3.182 for 3 degrees of freedom

Table 3. 3: Calibration Curve of PTX in ACN

Concentration (µg/ml)	Mean Absorbance ± SD (n=4)
2	0.093 ± 0.013
4	0.168 ± 0.004
6	0.251 ± 0.011
8	0.306 ± 0.011
10	0.375 ± 0.010
20	0.733 ± 0.013
30	1.086 ± 0.006
40	1.387 ± 0.005

Table 3. 4: Evaluation of accuracy & precision of the estimation method of PTX in ACN

Theoretical Concentration of PTX (µg/mL)	Determined Value (µg/mL) ± SD	Coefficient of variance (CV)	SEM ($SD/n^{1/2}$)	Confidence limits*
4	4.037 ± 0.074	0.005	0.037	4.037 ± 0.117
20	20.447 ± 0.498	0.248	0.249	20.447 ± 0.793
40	39.917 ± 0.152	0.023	0.076	39.919 ± 0.241

* At 95% Confidence level; t_{tab} = 3.182 for 3 degrees of freedom

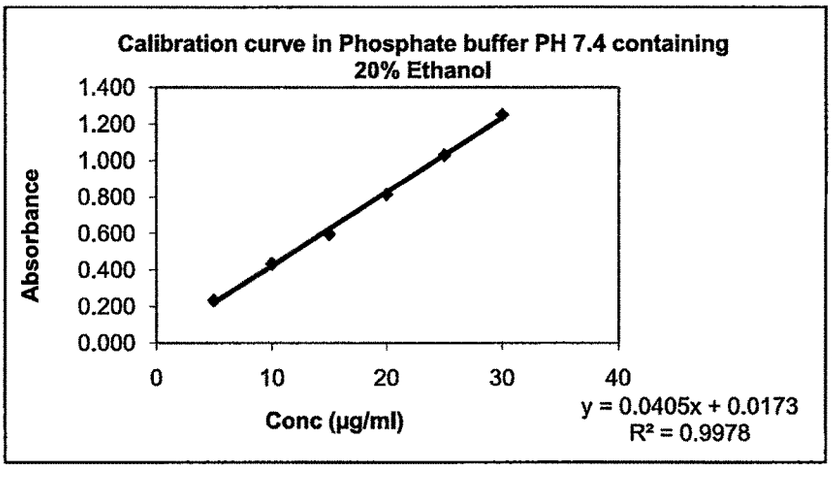

Figure 3. 4: Regressed calibration curve of PTX in pH 7.4 PBS containing 20% Ethanol

Table 3. 5: Calibration Curve of PTX in pH 7.4 PBS containing 20% Ethanol

Concentration (µg/ml)	Mean Absorbance ± SD (n=4)
5	0.233 ± 0.011
10	0.434 ± 0.017
15	0.597 ± 0.019
20	0.814 ± 0.026
25	1.030 ± 0.038
30	1.250 ± 0.016

Table 3. 6: Evaluation of accuracy & precision of the estimation method of PTX in pH 7.4 PBS 20% Ethanol

Theoretical Concentration of PTX (µg/mL)	Determined Value (µg/mL) ± SD	Coefficient of variance (CV)	SEM ($SD/n^{1/2}$)	Confidence limits*
5	5.117 ± 0.087	0.008	0.044	5.117 ± 0.139
20	19.950 ± 0.181	0.033	0.090	19.950 ± 0.288
30	29.630 ± 0.637	0.406	0.318	29.630 ± 1.013

* At 95% Confidence level; t_{tab} = 3.182 for 3 degrees of freedom

3.2.2 1st derivative spectroscopy for determination of PTX in PBCA NPs

Derivative spectrophotometry in the UV-Vis region is a useful technique in extracting qualitative and quantitative information from overlapping bands of the analyte and interferents due to incompletely resolved peaks. A number of studies have shown the advantage of higher selectivity of derivative spectrophotometry than normal (zero-order) spectrophotometry. Derivative spectra can be produced by processing the spectrophotometer output. The use of derivative spectra can increase the detection sensitivity of minor spectra features and reduce the error caused by the overlap of the analyte spectral band by interfering bands of other species in the sample. It is possible to measure the absolute value of the derivative of the sum curve at an abscissa value (wavelength) corresponding to a zero-crossing of one of the components in the mixture. This is termed a zero-crossing measure and can be applied to the first and second

derivatives. The zero-crossing derivative spectroscopic mode allows the resolution of interference and analytes by recording their derivative spectra at wavelengths at which one of the components exhibits no signal (Dixit and Ram, 1985; Eskandari et al., 2006). PTX in PBCA NPs was determined by 1st derivative spectroscopy as a strong interference of the polymer was found in the range of 220-250nm. The zero crossing point of polymer was found to be 248.5nm. At this wavelength the polymer did not exhibit any absorbance. Hence, linearity for 1st derivative of PTX spectra was obtained at this wavelength.

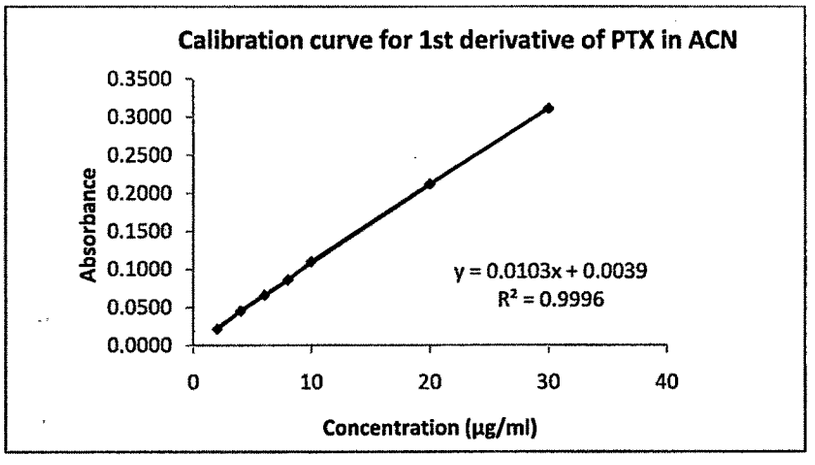

Figure 3. 5: 1st derivative regressed calibration curve of PTX in ACN

Table 3. 7: 1st Derivative Calibration Curve of PTX in ACN (λ_{max} = 248.5nm)

Concentration (µg/ml)	Mean Absorbance ± SD (n=4)
2	0.0215 ± 0.0007
4	0.0455 ± 0.0007
6	0.0580 ± 0.0000
8	0.0820 ± 0.0000
10	0.1100 ± 0.0000
20	0.2120 ± 0.0028
30	0.3110 ± 0.0014

Table 3. 8: Evaluation of accuracy & precision of the estimation method of 1st derivative of PTX in ACN

Theoretical Concentration of PTX (µg/mL)	Determined Value (µg/mL) ± SD	Coefficient of variance (CV)	SEM ($SD/n^{1/2}$)	Confidence limits*
4	4.040 ± 0.144	0.021	0.072	4.040 ± 0.229
20	20.363 ± 0.580	0.336	0.290	20.363 ± 0.922
30	40.993 ± 0.912	0.831	0.456	40.993 ± 1.451

* At 95% Confidence level; t_{tab} = 3.182 for 3 degrees of freedom

3.2.3 High Performance Liquid Chromatography

HPLC conditions

The drug content was determined using a HPLC system (Waters 2695 seperations module, USA). The HPLC system was composed of a UV-visible spectrophotometric detector (Waters 2487 Dual λ Absorbance detector, USA). The separation was performed on a C 18 150-4.6 HPLC column (Phenomenex Gemini C-18, 250 cm X 4.6mm, 5µm). Mobile phase consisted of acetonitrile: water mixture (70:30 v/v). The run time was 15 min and the retention time of paclitaxel was 4.5 min. UV detection wavelength was 230nm and mobile phase flow rate 1 ml/min. data processing was done using Empower Pro software (USA).

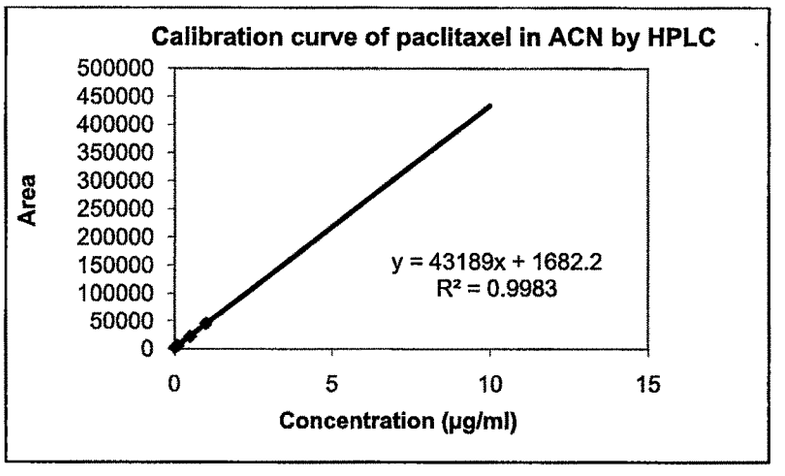

Figure 3. 6: Regressed calibration curve of PTX in ACN: water

Table 3. 9: Calibration Curve of PTX in ACN: water

Concentration (µg/ml)	Mean Absorbance ± SD (n=4)
0.01	1917
0.025	3203
0.05	4380
0.1	5886
0.5	21993
1	45489
10	438596

Table 3. 10: Evaluation of accuracy & precision of the estimation method of PTX in ACN: water

Theoretical Concentration of PTX (µg/mL)	Determined Value (µg/mL) ± SD	Coefficient of variance (CV)	SEM ($SD/n^{1/2}$)	Confidence limits*
0.01	0.011 ± 0.002	3.8E-06	0.001126	0.011 ± 0.004
0.1	0.133 ± 0.036	0.0013	0.020828	0.133 ± 0.049
10	10.047 ± 0.095	0.0089	0.054571	10.047 ± 0.234

* At 95% Confidence level; t_{tab} = 4.303 for 2 degrees of freedom

3.2.3 Estimation of PTX in rat plasma and tissue homogenates

Blood Collection and tissue homogenate preparation

Male Sprague Dawley rats were anaesthetized with ether and blood was collected from retro-orbital plexus of the eye using sterile glass capillary tube into glass vials containing 3%w/v sodium citrate solution as anticoagulant. The rats were sacrificed by cervical dislocation and dissected to collect the tissues such as brain, kidney, liver, lung, spleen and heart. The organs were then blotted using filter paper, weighed separately and homogenized, to a concentration of 5% w/v in water. The samples were centrifuged at 3000 rpm for 10 minutes and at 7000 rpm for 10 minutes at 4°C in a cooling centrifuge (Sigma, Osterode, Germany) to isolate the plasma and clear tissue homogenate respectively.

Construction of calibration plot in plasma and tissue homogenates

To 0.1 ml plasma or 1 ml tissue homogenate, required quantity of drug solution (from standards prepared in acetonitrile) was added to obtain the final concentrations of PTX ranging between 0.025 – 10 µg/ml. The contents were gently mixed to ensure uniform mixing and kept aside for 30min at room temperature. The samples were centrifuged at 4000rpm for 5 min and the supernatent was collected and estimated. All the estimations were carried out between 20°C - 27°C, and care was taken to prevent solvent evaporation at every stage of estimation. Calibration plot was constructed for the measured area against drug concentration. Accuracy and precision of the method was determined by performing recovery studies after addition of PTX in plasma and tissues in triplicate.

Accuracy and Precision

In order to determine the accuracy and precision of the developed method, known amounts of PTX at low medium and high concentration (0.01, 0.1 and 1 µg/ml) were subjected to recovery studies as per the procedure described earlier. The results obtained are tabulated in table 4.16.

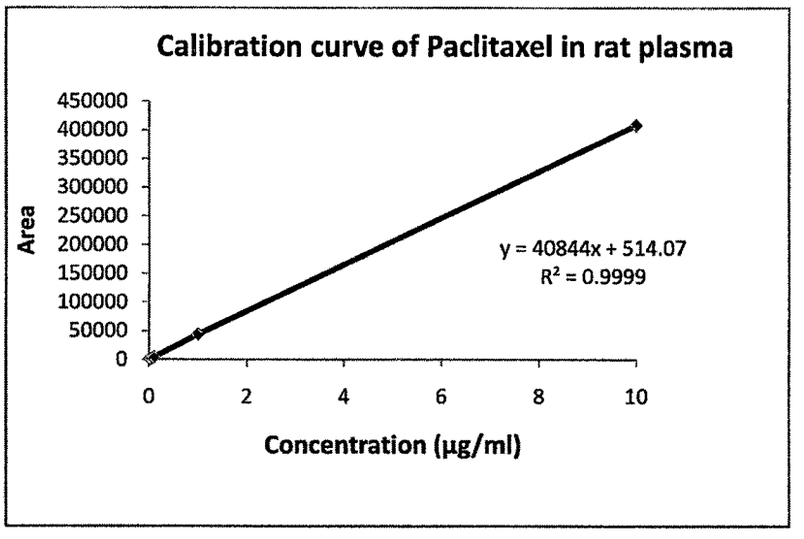

Figure 3. 7: Regressed calibration curve of PTX in rat plasma

Table 3. 11: Calibration Curve of PTX in rat plasma

Concentration (µg/ml)	Mean Area ± SD (n=3)
0.025	1072 ± 44.117
0.05	1907 ± 37.590
0.1	4072 ± 112.308
1	43777 ± 89.213
10	408721 ± 177.164

Table 3. 12: Evaluation of accuracy & precision of the estimation method of PTX in rat plasma

Theoretical Concentration of PTX (ng/mL)	Determined Value (µg/mL) ± SD	Coefficient of variance (CV)	SEM ($SD/n^{1/2}$)	Confidence limits*
0.025	0.0228 ± 0.0024	5.89E-06	0.001401	0.0228 ± 0.006
0.1	0.0820 ± 0.0045	0.000021	0.00264	0.0820 ± 0.011
1	0.8067 ± 0.0737	0.005433	0.04255	0.8067 ± 0.183

* At 95% Confidence level; t_{tab} = 4.303 for 2 degrees of freedom

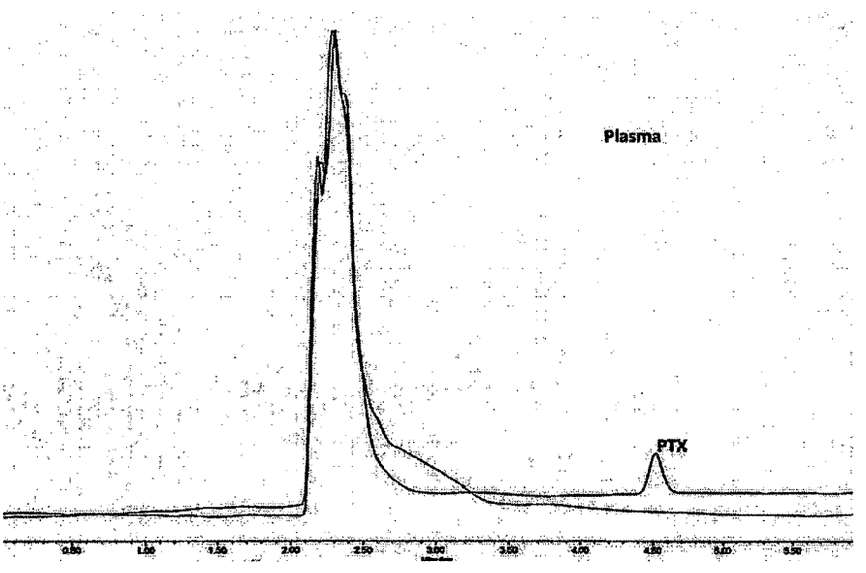

Figure 3. 8: Overlay chromatogram of blank plasma and plasma spiked with PTX

Table 3. 13: Mean Area ± SD obtained from the calibration curve of estimation of PTX in tissue homogenates of rat

Conc. (µg/mL)	Mean Area ± S.D (in lung homogenate)	Mean Area ± S.D (in heart homogenate)	Mean Area ± S.D (in spleen homogenate)	Mean Area ± S.D (in liver homogenate)	Mean Area ± S.D (in kidney homogenate)	Mean Area ± S.D (in brain homogenate)	Mean Area ± S.D (in tumor homogenate)
0.025	1768 ± 19.3	1967 ± 10.7	2055 ± 32.9	2008 ± 41.2	1934 ± 45.2	1879 ± 24.3	2098 ± 68.4
0.05	3568 ± 87.3	3615 ± 23.5	4885 ± 95.3	3788 ± 76.3	5480 ± 38.6	4290 ± 85.4	4276 ± 94.7
0.1	17840 ± 43.5	14876 ± 49.1	12876 ± 69.1	11897 ± 108.4	12980 ± 79.3	12837 ± 93.9	11869 ± 100.3
0.5	28756 ± 119.6	26237 ± 39.5	28434 ± 109.6	32195 ± 98.7	29089 ± 124.7	29108 ± 173.1	30473 ± 214.2
1	69481 ± 104.1	53467 ± 198.4	54672 ± 153.4	53729 ± 128.5	52839 ± 195.3	51987 ± 108.4	50385 ± 158.4
5	277137 ± 92.3	239773 ± 169.3	240319 ± 176.3	240720 ± 214.4	239765 ± 153.8	240894 ± 124.9	243657 ± 117.8

Regression equation for PTX in lung homogenate : $y = 54582x + 5703$; $R^2 = 0.996$

Regression equation for PTX in heart homogenate : $y = 47193x + 4153$; $R^2 = 0.998$

Regression equation for PTX in spleen homogenate : $y = 47258x + 4632$; $R^2 = 0.999$

Regression equation for PTX in liver homogenate : $y = 47342x + 4722$; $R^2 = 0.998$

Regression equation for PTX in kidney homogenate : $y = 47101x + 4614$; $R^2 = 0.999$

Regression equation for PTX in brain homogenate : $y = 47417x + 4081$; $R^2 = 0.999$

Regression equation for PTX in tumor homogenate : $y = 47992x + 3734$; $R^2 = 0.999$

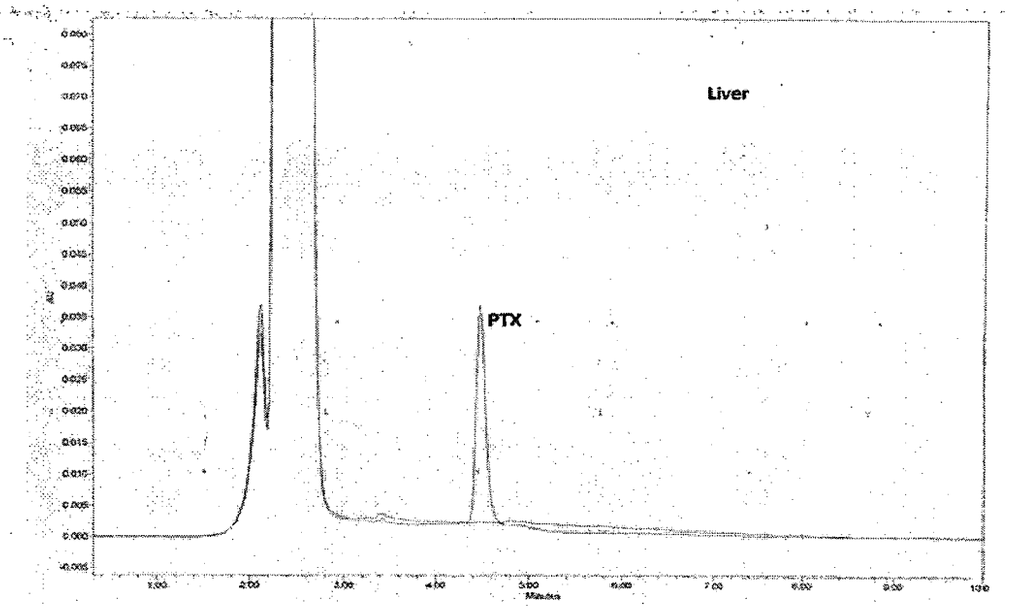

Figure 3. 9: Overlay chromatogram of blank liver homogenate and liver homogenate spiked with PTX

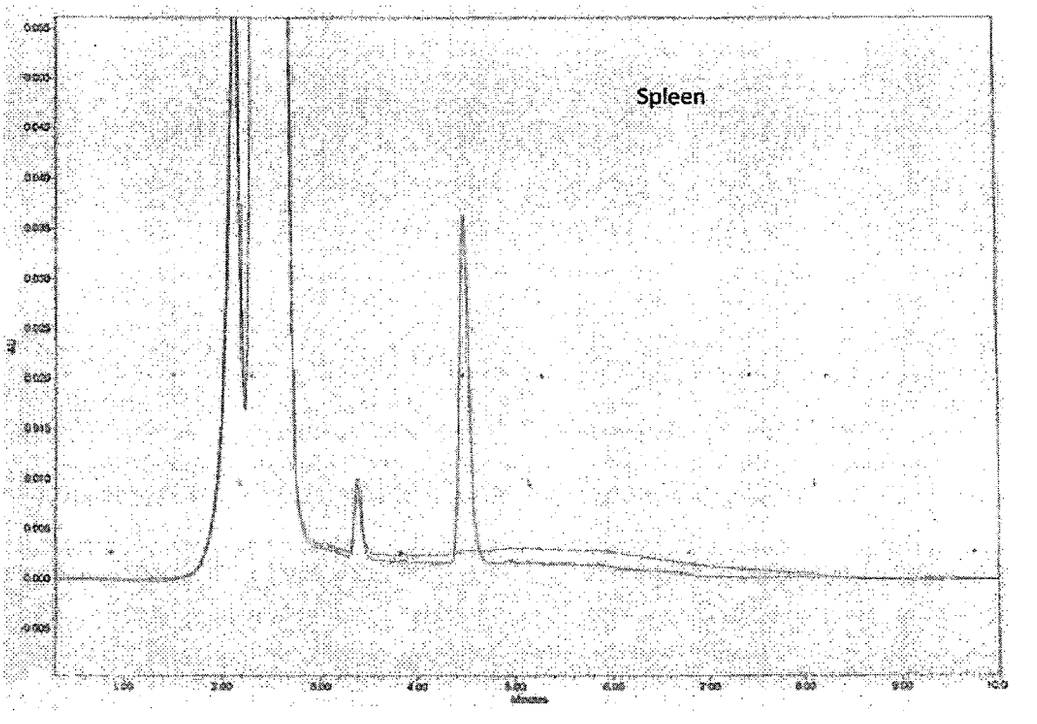

Figure 3. 10: Overlay chromatogram of blank spleen homogenate and spleen homogenate spiked with PTX

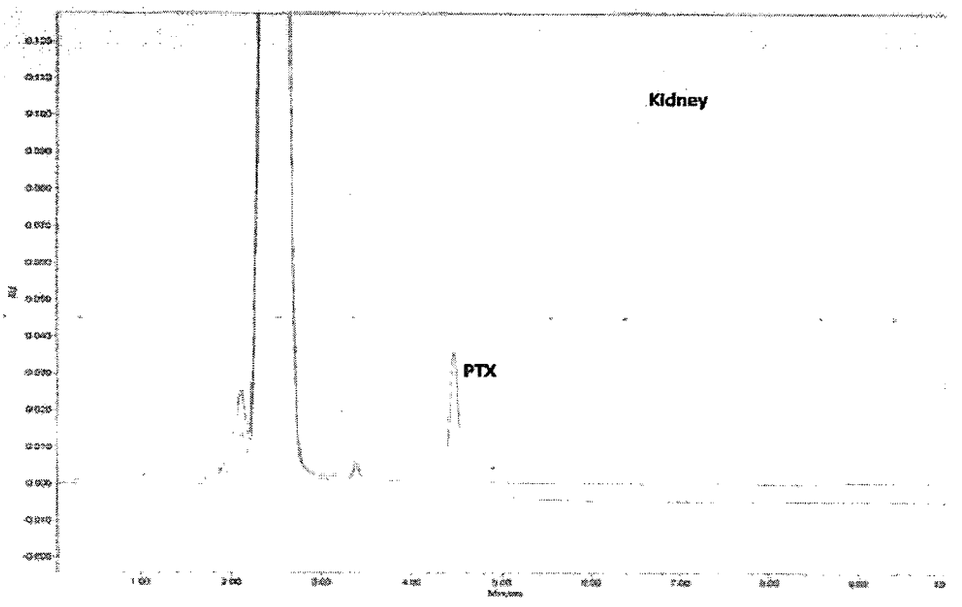

Figure 3. 11: Overlay chromatogram of blank kidney homogenate and kidney homogenate spiked with PTX

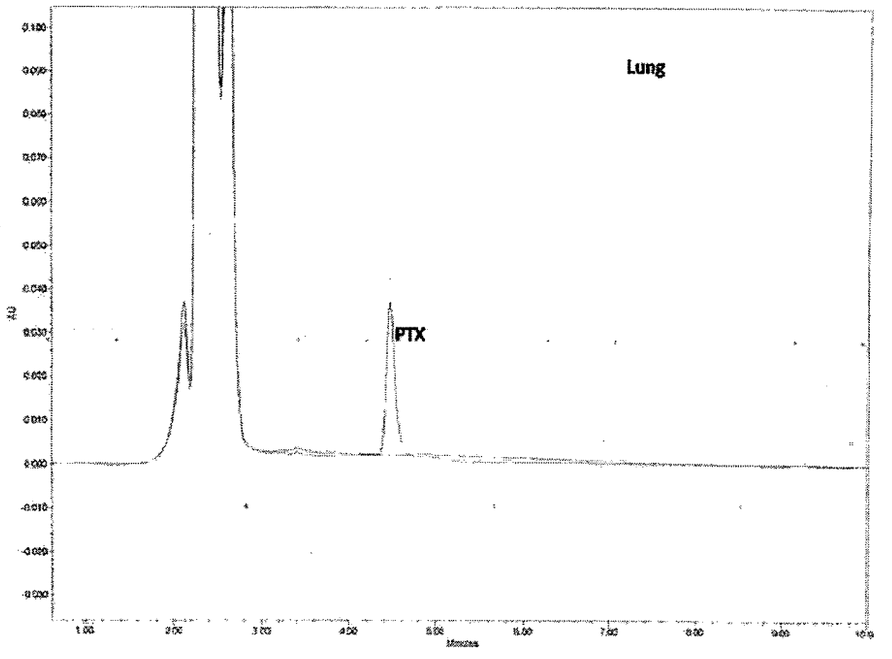

Figure 3. 12: Overlay chromatogram of blank lung homogenate and lung homogenate spiked with PTX

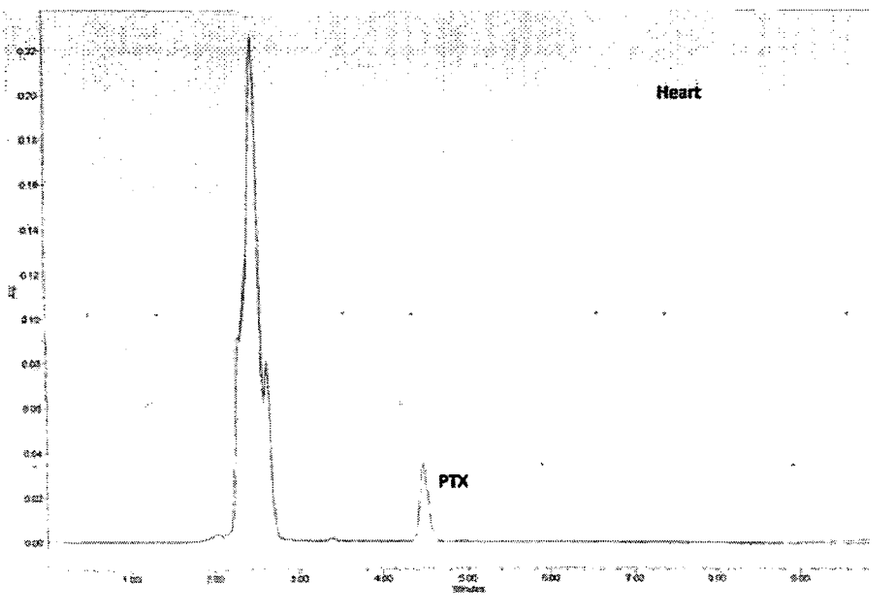

Figure 3. 13: Overlay chromatogram of blank heart homogenate and heart homogenate spiked with PTX

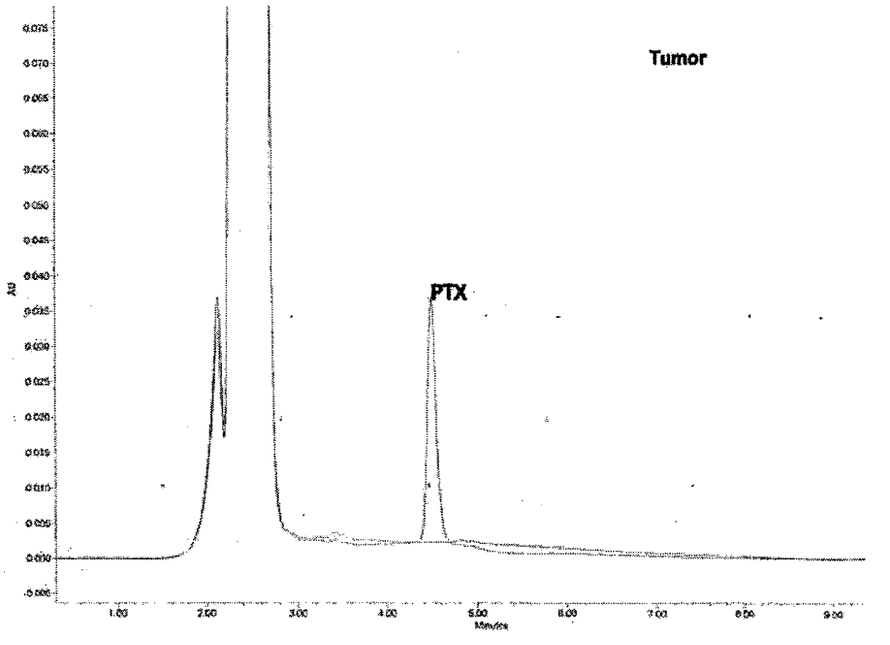

Figure 3. 14: Overlay chromatogram of blank tumor homogenate and tumor homogenate spiked with PTX

Table 3. 14: Determination of accuracy and precision of estimation of PTX in tissue homogenates of rat

Theoretical Concentration of PTX (µg/mL)	Determined Value (ng/mL) ± SD	Coefficient of variance (CV)	SEM ($SD/n^{1/2}$)	Confidence limits
Lung Homogenate				
0.1	0.099 ± 0.019	0.00035	0.01084	0.099 ± 0.046
0.5	0.502 ± 0.033	0.00110	0.01914	0.502 ± 0.082
1.0	0.940 ± 0.111	0.01240	0.06429	0.940 ± 0.276
Heart Homogenate				
0.1	0.088 ± 0.010	0.00010	0.00578	0.088 ± 0.024
0.5	0.460 ± 0.082	0.00670	0.04726	0.460 ± 0.203
1.0	0.876 ± 0.073	0.005433	0.042558	0.876 ± 0.183
Spleen Homogenate				
0.1	0.0803 ± 0.007	0.00004	0.00376	0.080 ± 0.016
0.5	0.4600 ± 0.072	0.00520	0.04163	0.460 ± 0.179
1.0	0.9100 ± 0.020	0.00040	0.01155	0.910 ± 0.049
Liver Homogenate				
0.1	0.0830 ± 0.004	0.00002	0.00231	0.083 ± 0.009
0.5	0.4400 ± 0.062	0.00390	0.03606	0.062 ± 0.155
1.0	0.9900 ± 0.056	0.00310	0.03215	0.056 ± 0.138
Kidney Homogenate				
0.1	0.0847 ± 0.009	0.00008	0.00504	0.084 ± 0.021
0.5	0.4667 ± 0.087	0.00763	0.05044	0.466 ± 0.217
1.0	0.8977 ± 0.035	0.00125	0.02038	0.897 ± 0.087
Tumor Homogenate				
0.1	0.0783 ± 0.004	0.00002	0.00233	0.078 ± 0.010
0.5	0.4367 ± 0.059	0.00343	0.03383	0.436 ± 0.145
1.0	0.9033 ± 0.025	0.00063	0.01453	0.903 ± 0.062

* At 95% Confidence level; t_{tab} = 4.303 for 2 degrees of freedom

3.3 Estimation of coumarin-6

3.3.1 Estimation of coumarin-6 in formulations

All fluorimetric estimations were performed on a Shimadzu RF-540 spectrofluorometer (Shimadzu Coporation, Japan) equipped with a xenon lamp. The various experimental conditions like the slit width for excitation (kept at 3) and emission (kept at 5) and the excitation and emission wavelengths ($\lambda_{excitation}$ = 430nm; $\lambda_{emission}$ = 485) were optimized.

Preparation of Calibration Plot in ACN

Stock solution of coumarin-6 in acetonitrile was prepared by accurately weighing 10mg of coumarin-6 in 100mL of solvent. After ensuring that the coumarin-6 has totally dissolved, suitable aliquots of the 100µg/mL stock solution of coumarin-6 was pipetted into 10mL volumetric flasks. The volume was made upto 10mL using the same solvent. The contents were shaken well and the relative fluorescence intensity was measured setting the $\lambda_{excitation}$ at 430nm and the corresponding $\lambda_{emission}$ peak intensity was measured at 485nm (slit widths as mentioned above) using a Shimadzu RF-540 spectrofluorometer (Shimadzu Corporation, Japan) against suitable blank. The above procedure was repeated 4 times and the mean relative fluorescence intensity values were determined. The mean relative fluorescence intensity obtained tabulated in Table 15. The $\lambda_{emission}$ peaks of coumarin-6 in acetonitrile are shown in Figure 3.16.

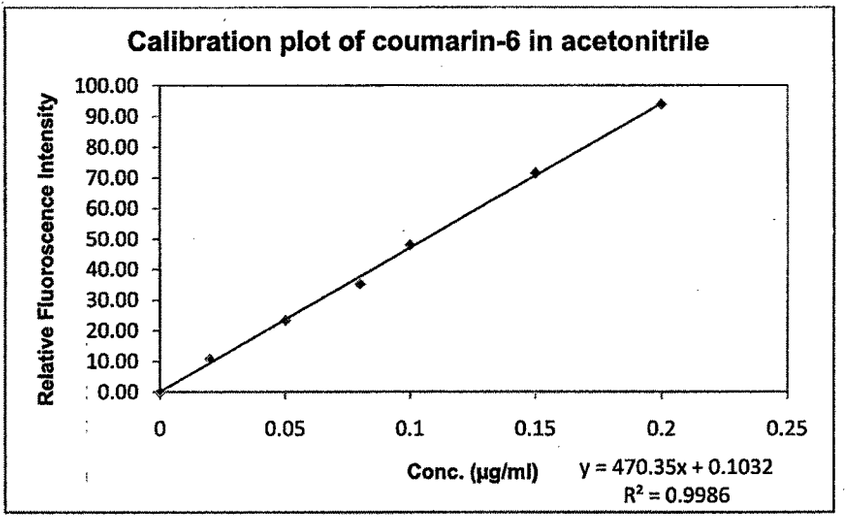

Figure 3. 15: Regressed calibration curve of coumarin-6 in ACN

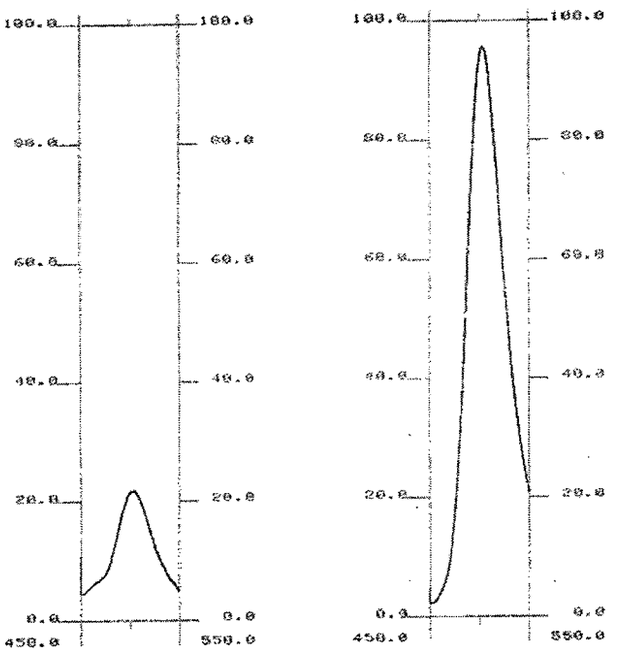

Figure 3. 16: Emission peaks of coumarin-6

Accuracy and Precision

In order to determine the accuracy and precision of the developed method, known amounts of coumarin-6 (50, 100 and 200ng/mL) are subjected to recovery studies as per the procedure described earlier. Obtained results are tabulated in Table 16.

Table 3. 15: Calibration Curve of coumarin-6

Concentration (ng/ml)	Mean Fluorescence ± SD (n=3)
0.02	10.73 ± 0.41
0.05	23.33 ± 0.60
0.08	35.23 ± 0.65
0.10	48.13 ± 0.55
0.15	71.53 ± 0.87
0.20	93.97 ± 0.80

Table 3. 16: Evaluation of accuracy & precision of the estimation method of coumarin-6 in ACN

Theoretical Concentration of coumarin-6 (µg/mL)	Determined Value (µg/mL) ± SD	Coefficient of variance (CV)	SEM ($SD/n^{1/2}$)	Confidence limits*
0.050	0.0490 ± 5.7E-05	0.117907	3.33E-09	0.050 ± 0.001
0.100	0.1100 ± 0.01	1E-04	0.005774	0.100 ± 0.024
0.200	0.1967 ± 0.0057	3.33E-05	0.003333	0.200 ± 0.014

* At 95% Confidence level; t_{tab} = 4.303 for 2 degrees of freedom

3.3.2 Estimation of coumarin-6 in cell lysate

C6 rat glioma cells were seeded at a density of 1 X 10^4 cells/well in 96 well plate (Nunclone®surface, Nunc, Roskilde, Denmark). Allow the cells to attach overnight. The cells were lysed with 100 µl of cell lysis buffer (Promega, Madison, USA). 100 µl of standard solutions (0.075 to 20 µg/ml) of coumarin-6 prepared in acetonitrile were added into the plates and read at excitation and emission wavelength of 430nm and 485nm respectively on microplate reader (Synergy HT, Biotek, USA).

Accuracy and Precision

In order to determine the accuracy and precision of the developed method, known amounts of coumarin-6 (0.1, 0.5 and 5.0 µg/mL) as subjected to recovery studies as per the procedure described earlier. Obtained results are tabulated in Table 18.

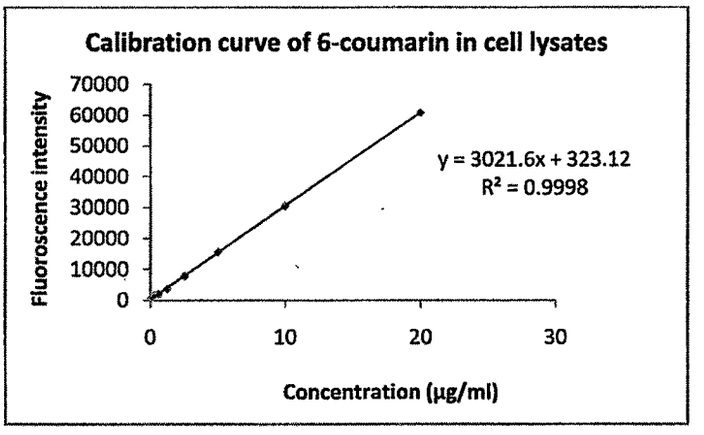

Figure 3. 17: Regressed calibration curve of coumarin-6 in ACN

Table 3. 17: Calibration Curve of coumarin-6

Concentration (µg/ml)	Mean Fluorescence ± SD (n=3)
0.075	652.5 ± 4.94
0.150	889.0 ± 4.24
0.300	1550.0 ± 2.82
0.600	1989.5 ± 6.36
1.250	3569.5 ± 3.53
2.500	7833.5 ± 2.12
5	15751.0 ± 2.82
10	30355.5 ± 4.94
20	60804 ± 2.43

Table 3. 18: Evaluation of accuracy & precision of the estimation method of coumarin-6 in cell lysate

Theoretical Concentration of coumarin-6 (µg/mL)	Determined Value (µg/mL) ± SD	Coefficient of variance (CV)	SEM ($SD/n^{1/2}$)	Confidence limits*
0.1	0.093 ± 0.015	0.00016	0.00722	0.093 ± 0.031
0.5	0.476 ± 0.015	0.00023	0.00882	0.476 ± 0.037
5.0	4.720 ± 0.067	0.00442	0.03844	4.720 ± 0.165

* At 95% Confidence level; t_{tab} = 4.303 for 2 degrees of freedom

3.4 Estimation of residual PVA

The amount of PVA associated with nanoparticles was determined by a colorimetric method based on the formation of a colored complex between two adjacent hydroxyl groups of PVA and an iodine molecule (Joshi et al, 1979). For a calibration plot of PVA prepare a stock solution of 1000µg/ml from which different aliquotes were taken to get the final concentrations (10-250 µg/ml). To 5ml of each sample, 3 ml of a 0.65 M solution of boric acid, 0.5 ml of a solution of I_2/KI (0.05 M/0.15 M), and 1.5 ml of distilled water were added. Finally, the absorbance of the samples was measured at 690 nm after 15 min incubation. A standard plot of PVA was prepared under identical conditions.

Table 3. 19: Calibration Curve of PVA

Concentration (µg/ml)	Mean Absorbance ± SD (n=3)
10	0.045 ± 0.36
20	0.094 ± 0.78
30	0.143 ± 0.86
40	0.191 ± 1.05
50	0.232 ± 0.24
100	0.468 ± 0.92
250	1.210 ± 1.26

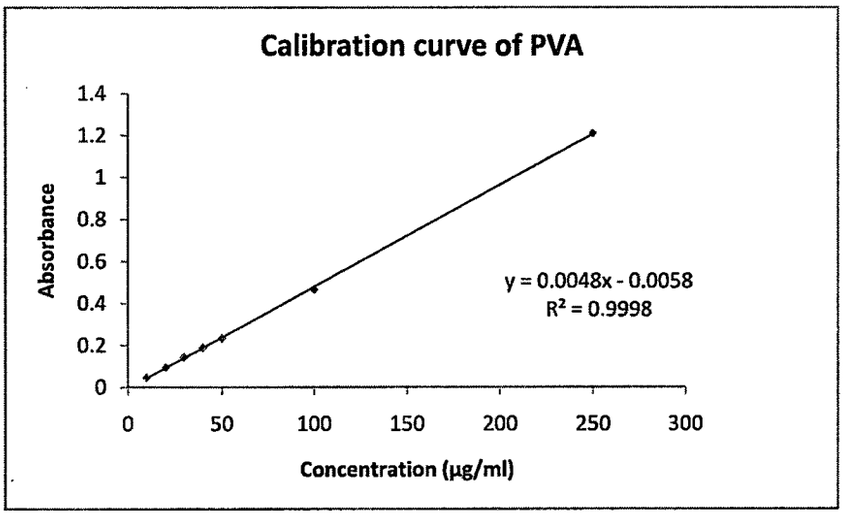

Figure 3. 18: Regressed calibration curve for determination of residual PVA

3.5 Determination of protein (Transferrin) by BCA method

Determination of protein was done using Protien estimation kit (Genei, Banglore). Protein Assay based on bicinchoninic acid (BCA) is a most sensitive and detergent compatible method for the colorimetric detection and quantitation of total protein. This method is a combination of the well-known biuret reaction, the reduction of Cu^{2+} to Cu^{1+} by protein in an alkaline medium and the highly sensitive and selective colorimetric detection of the cuprous cation (Cu^{2+}) with reagent containing Bichinconinic acid (Smith et al). Transferrin has the macromolecular structure of protein, the number of peptide bonds and the presence of amino acids (Wiechelman et al). Two molecules of chelate BCA with one

cuprous ion form a purple-colored reaction product of this assay. This water-soluble complex exhibits a strong absorbance at 562 nm. The calibration curve was plotted according to the manufacturer's instructions.

BCA-Protein Reaction

1. Protein (peptide bonds) + Cu^{2+} tetradentate- Cu^{1+} complex
2. Cu^{1+} + 2 Bichinchoninic Acid BCA- Cu^{1+} complex (purple colored, read at 562nm)

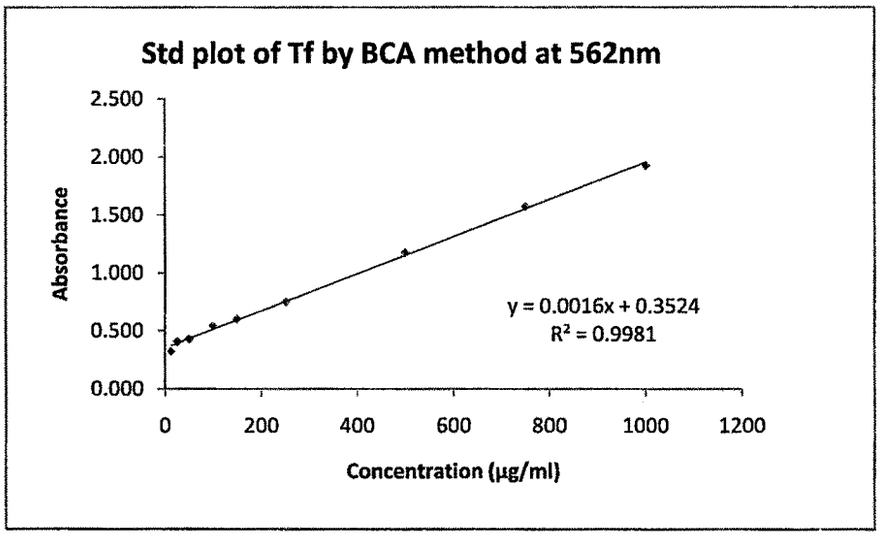

Figure 3. 19: Regressed calibration curve of Tf by BCA method

Table 3. 20: Calibration Curve of Tf by BCA method

Concentration (µg/ml)	Mean Absorbance ± SD (n=4)
12.5	0.324 ± 0.0063
25	0.404 ± 0.0021
50	0.426 ± 0.0070
100	0.538 ± 0.0113
150	0.601 ± 0.0127
250	0.749 ± 0.0275
500	1.175 ± 0.0494
750	1.570 ± 0.0565
1000	1.925 ± 0.1073

References

Dixit L, Ram S. Quantitavie analysis by derivative electronic spectroscopy. Appl. Spectrosc. Rev., 1985, 21, 311-418.

Eskandari H, Saghseloo AG, Chamjangali MA. First- and Second-Derivative Spectrophotometry for Simultaneous Determination of Copper and Cobalt by 1-(2-Pyridylazo)-2-naphthol in Tween 80 Micellar Solutions. Turk J Chem 30 (2006) 49-63.

Joshi DP, Lan-Chun-Fung YL, Pritchard JW. Determination of poly (vinyl alcohol) via its complex with boric acid and iodine. Anal. Chim. Acta 104 (1979) 153–160.

Ojeda CB, Rojas FS, Pavon JM, Recent developments in derivative ultraviolet/visible absorption spectrophotometery. Talanta (1995), 42, 1195.